ROZPRAWY INŻYNIERSKIE • ENGINEERING TRANSACTIONS • 31, 3, 341–360, 1983
Polska Akademia Nauk • Instytut Podstawowych Problemów Techniki

ON THE RATE SENSITIVITY OF COAL

J. R. KLEPACZKO (WARSZAWA)

This paper describes the development of quasi-static and dynamic techniques applicable to compression testing of coal over a strain rate range of $\dot{\varepsilon}_{\min} \approx 1.3 \times 10^{-4}\ s^{-1}$ to $\dot{\varepsilon}_{\max} \approx 2 \times 10^{3}\ s^{-1}$. At low and moderate strain rates a closed loop machine was used, while at high strain rates was accomplished with a newly-developed Hopkinson pressure bar apparatus. The loading direction was perpendicular to the specimen bedding plane (Z-direction) for all of the tests. Test results show a strong dependence of ultimate or crushing strength on the rate of deformation for the high region ($\dot{\varepsilon} \approx 10^{3}\ s^{-1}$), whereas at low and intermediate strain rates the strength values seem to be rate insensitive.

1. Introduction

Coal still remains a main source of energy for coming decades and well into the twenty first century. It recently has received renewed interest due to new technologies such as in-situ coal gasification, coal conversion by liquefaction and others. Although standard mechanical testing of coal is well developed [1, 5], more sophisticated experimental techniques have been employed recently to test coal under different conditions. Since it is well known that all gasification schemes require proper coal bed preparation by cracking and fragmenting, an explosive technique is usually applied to produce such a condition.

Thus it is desirable to obtain some information on the behavior of coal under impact loading and relate the data to quasi-static behavior. Literature on the mechanical properties of coal do not include much information on the dynamic response of this material. Fracture toughness behavior of coal under impact loading is also of great interest.

This paper, however, concentrates on the behavior of coal tested in compression. It is assumed that all testing is performed under condition of uniaxial stress. Such an approach may be helpful in the formulation of a constitutive relation for coal. The effect of the hydrostatic component of stress on the rate sensitivity of coal should be explored later. Coal is also sensitive to the hydrostatic component of stress. These features are observed in all rocks and rock-like materials [3, 4].

In the literature available very few data have in fact been published on the visco-elastic and visco-plastic properties of coal. As to visco-elastic properties, it is known that coal exhibits time-dependent behavior affecting elastic constants [1]. Creep behavior was also observed during quasi-static compression tests [1].

In addition to visco-elastic properties, shock compression measurements on coal have shown its high strain rate sensitivity [2]. The uniaxial strain shock compression experiments provided clear evidence that coal is not only a highly compressible material, but also shows a strong dependence of stress-strain characteristics on strain rate.

Because of the significance of the time-dependent behavior of coal, a more systematic experimental study was undertaken to enhance scattered data on this subject reported in literature.

2. Quasi-static properties of coal in compression

To complete the whole strain rate spectrum several strain rates are usually applied. Part of this spectrum can be obtained using standard closed loop hard machines. However, higher strain rates, usually in excess of $\dot{\varepsilon}=1\ s^{-1}$, can be obtained only with the aid of specially designed impact devices.

Since it is desirable to use always the same specimen geometry, tailored for quasi-static as well as for impact testing, a short disc shape has been accepted. Coal specimens of diameter $D=25$ mm and height $L=12.4$ mm were used throughout the testing. For such specimen geometry the height to diameter ratio equal 0.5 was the most optimal in compression impact experiment [21].

The order of maximum fracture strain ε_{fm} for coal in compression tests is about 2×10^{-2}. Thus the maximum displacement U_{max} to crush the coal specimen is ~0.25 mm, and as a consequence an accurate determination of Young's modulus requires a displacement resolution in the order of $\Delta U=2.5\times10^{-4}$ mm. The required displacement resolution was obtained by constructing a device for the precision compression tests. Figure 1 shows a schematic of this device mounted into standard closed loop testing machine. A disc specimen is inserted between the upper and lower platens, and the relative displacement U between the platens is monitored by two *DCDT* displacement transducers. Any platen tilt is eliminated automatically by proper elastical connections. The lower platen is supported only on one steel ball, allowing the platen to accommodate to the specimen. In this way any stress concentrations on the specimen edges are eliminated, an important feature in the testing of semi-brittle material like coal.

After conditioning the signals from both the load cell and the two *DCDT*, it is possible to obtain a force-displacement diagram $P(\Delta L)$, where reduction of the specimen height ΔL is positive. An alternate approach, applicable for short time loading, uses a digital transient recorder to obtain both P and ΔL as functions of time; $P(t)$ and $\Delta L(t)$. Due to the high resolution of the measuring system and the small displacement ΔL_{max} necessary to crush coal specimens, the compliance of the mechanical system, more exactly the stiffness of both platens, must be taken into consideration.

For this purpose the procedure for the determination of compression characteristics of coal has been established. This method, called the precision compression

test, has been used in this paper for all quasi-static tests. A more exact description of this procedure can be found in [6].

As a beginning, coal description and specimen preparation procedures will be provided. All disc specimens were obtained from a Nova Scotia (1) coal, its physical properties given in [5]. The test specimens were cut with the aid of a coring

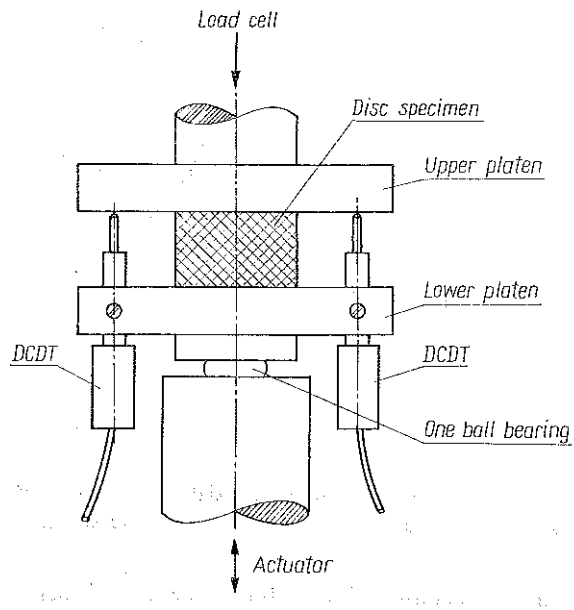

FIG. 1. Schematic layout of the device for precision compression test.

rig of ~25 mm diameter and next they were cut to ~12.5 mm in length. The ends were finished by a grinding belt-sander to obtain parallelism better than ±0.02 mm. The parallelism is very important since 0.02 mm introduces an error into strain measurement $W \approx 1.6 \times 10^{-3}$.

Three series of specimens were prepared from three orthogonal directions with respect to the bedding plane. The bedding plane is assumed to lay on the (X, Y) plane, where X is the direction along the seam, and direction Y coincides with the seam width. Consequently, direction Z is perpendicular to the seam plane and neglecting curvature is parallel to the surface of the earth.

Controlled strain rate tests were performed in compression for all three directions at strain rate $\dot{\varepsilon} = 1.3 \times 10^{-4}\ s^{-1}$ with a closed loop testing machine. Specimen faces are lubricated before each test with a MoS_2 base lubricant. For each direction at least five good tests have been completed.

Due to a high resolution in strain recording it is demonstrated that the complete stress-strain curve for coal in uniaxial compression consists basically of four regions. Such a curve always displays an S-shape, as shown schematically in Fig. 2. The

(1) The coal was provided by Noval Technologies, Ltd.

first region, observed at relatively low stresses begins from the origin and is curved due to the high compressibility of coal. Within this region the tangent modulus $d\sigma/d\varepsilon$ slightly increases. The second region, observed at medium stresses, is char-

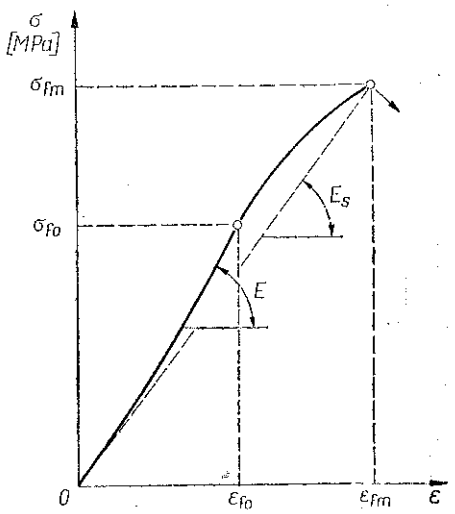

FIG. 2. Stress-strain curve observed for coal in uniaxial compression; E—Young's modulus; E_s—secant modulus; ε_{fm}—maximum fracture stress.

acterized by an almost constant value of the tangent modulus. This is the highest modulus observed and throughout this paper has been defined as Young's modulus, E

$$E=\left(\frac{d\sigma}{d\varepsilon}\right)_{\max}.$$

Both regions are basically elastic und exhibit a small hysteresis loop. The third region strarts after exceeding the stress level σ_{f0}. This is the region characteristic of microcracking and of progressive fracturing in a stable manner. Due to the process of stable cracking, a substantial decrease of tangent modulus is observed. There is also a considerable hysteresis observed during unloading. Phenomenologically, this region can be recognized as "plasticity with nonlinear strain hardening". In this region the maximum strength σ_{fm} is attained. The fourth region begins just shortly after the maximum stress is reached, when the system becomes unstable and the specimen starts to disintegrate. For the case of a stiff testing machine, the specimen fails gradually as cracks extend further, with its load carrying capacity decreasing relatively quickly to a total specimen collapse and complete disintegration. This region, however, will not be analyzed in this paper.

After defining characteristic points on the stress-strain curve, the following quantities can be determined from each test:

i) Young's modulus $E=(d\sigma/d\varepsilon)_{\max}$;

ii) Secant modulus $E_s=\sigma_{fm}/\varepsilon_{fm}$;

iii) initiation point of microcracking ($\sigma_{fo}, \varepsilon_{fo}$);

iv) fracture point ($\sigma_{fm}, \varepsilon_{fm}$).

The crushing parameters which have been determined for Z direction, as defined in Fig. 2, are given in Table 1. The whole stress-strain diagrams for five tests are shown in Fig. 3. Average values for ($\sigma_{fo}, \varepsilon_{fo}$) and ($\sigma_{fm}, \varepsilon_{fm}$) at $\dot{\varepsilon}=1.3\times10^{-4}$ are also given in Table 1. Comparison of ε_{fo} to ε_{fm} shows that the nonlinear portion of the stress-strain diagram takes about one third of the total strain to fracture

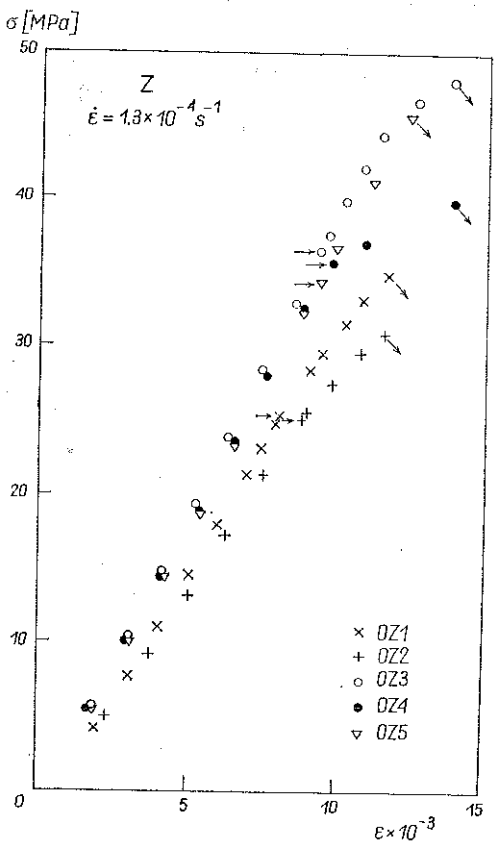

FIG. 3. Stress-strain characteristics for coal in Z direction, $\dot{\varepsilon}=1.3\times10^{-4}\,s^{-1}$.

Table 1. Crushing parameters for coal at $\dot{\varepsilon}=1.3\times10^{-4}\,s^{-1}$; $\bar{\sigma}_{fo}$, $\bar{\varepsilon}_{fo}$ and $\bar{\sigma}_{fm}$ are averaged values from five tests.

Direction	Specimen	$\varepsilon_{fo}\times10^{-3}$	σ_{fo}[MPa]	$\varepsilon_{fm}\times10^{-3}$	σ_{fm}[MPa]	Average value
Z	0Z1	8.03	25.45	11.69	35.03	$\bar{\varepsilon}_{fo}=9.17\times10^{-3}$
	0Z2	8.78	25.19	11.55	30.89	$\bar{\sigma}_{fo}=31.94$MPa
	0Z3	9.32	36.48	13.86	48.11	
	0Z4	9.75	35.76	13.90	39.84	$\bar{\varepsilon}_{fm}=12.68\times10^{-3}$
	0Z5	9.95	36.80	12.40	45.72	$\bar{\sigma}_{fm}=39.92$MPa

ε_{fm}. The important conclusion can be reached that the "hardening" portion of the stress-strain diagram must be taken into consideration during formulation of a constitutive relation for coal in compression. The second observation is that the beginning of microcracking takes place at about 0.8 of the crushing stress σ_{fm}. Therefore, coal may be loaded in compression without substantial cracking detected by mechanical testing up to about 0.8 of its strength. It is to be remembered that the mean compressive strength decreases with increasing volume of stressed material [1]. Thus the value 0.8 should be understood as a tentative.

To reveal the influences of the time factor in uniaxial compression of coal, further tests were carried out at higher strain rates. Again, the controlled strain rate tests were performed at $1.7\times10^{-2}\ s^{-1}$ and $\sim2.0\ s^{-1}$ with the same closed loop testing machine supplying the axial load. The same device for the precision

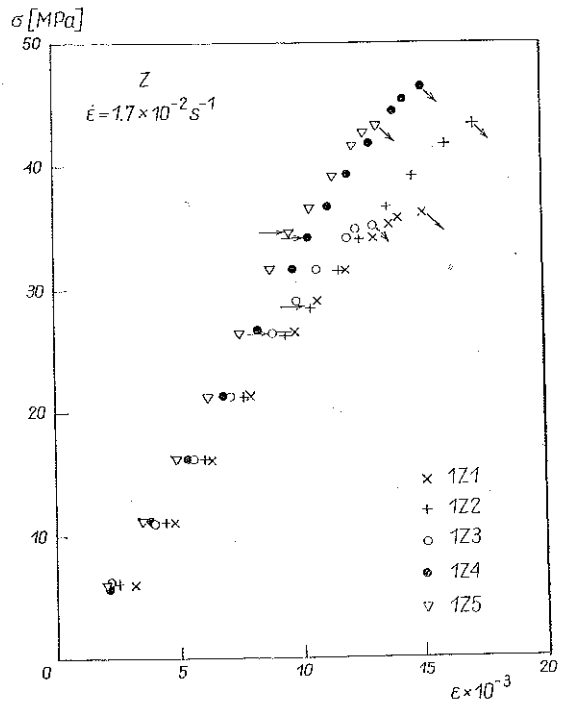

FIG. 4. Stress-strain characteristics for coal in Z direction, $\dot{\varepsilon}=1.7\times10^{-2}\ s^{-1}$.

Table 2. Crushing parameters for coal at $\dot{\varepsilon}=1.7\times10^{-2}\ s^{-1}$.

Direction	Specimen	$\varepsilon_{fo}\times10^{-3}$	σ_{fo}[MPa]	$\varepsilon_{fm}\times10^{-3}$	σ_{fm}[MPa]	Average value
Z	1Z1	9.69	26.51	15.1	36.19	$\bar{\varepsilon}_{fo}=9.62\times10^{-3}$
	1Z2	10.4	28.48	17.2	43.73	$\bar{\sigma}_{fo}=30.04$ [MPa]
	1Z3	8.77	26.51	13.0	35.13	$\bar{\varepsilon}_{fm}=14.70\times10^{-3}$
	1Z4	10.3	34.44	15.0	46.37	$\bar{\sigma}_{fm}=40.92$ [MPa]
	1Z5	8.95	34.54	13.2	43.17	

compression tests was used (Fig. 1) with the same specimen geometry. Specimen faces were lubricated with the same lubricant. Thus the only factor which was changed was the strain rate.

At strain rate $\dot{\varepsilon}=1.7\times10^{-2}\ s^{-1}$ five good tests were completed and stress-strain curves calculated. The same compliance function was used to calculate stresses and strains of a specimen [6]. The final results of these tests are shown in Fig. 4 and in Table 2.

The next series of tests were performed at approximately $\dot{\varepsilon}=2.0\ s^{-1}$, and stress--strain characteristics for six specimens are shown in Fig. 5 and in Table 3.

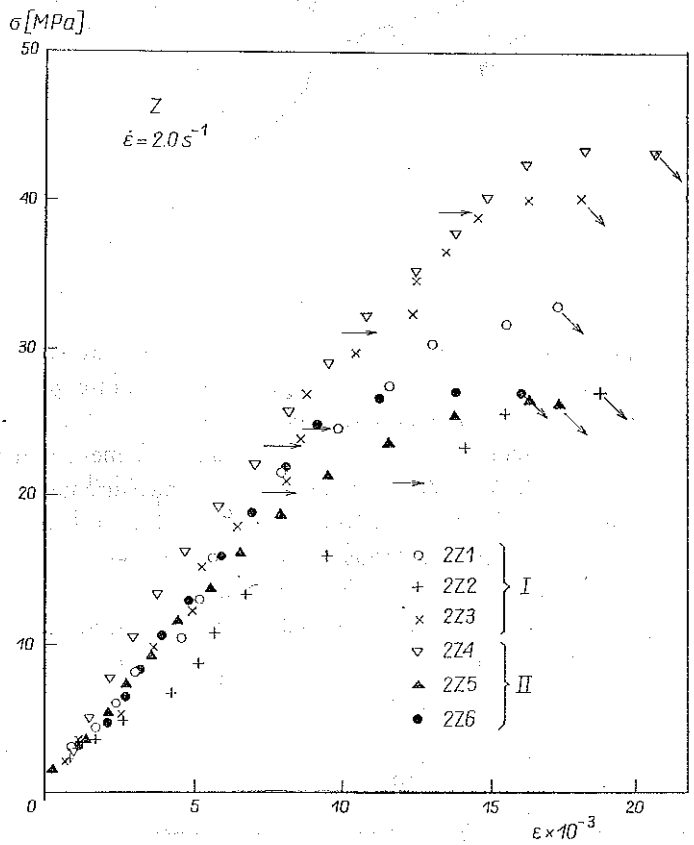

FIG. 5. Stress-strain characteristics for coal in Z direction, $\dot{\varepsilon}\approx2.0\ s^{-1}$.

Table 3. Crushing parameters for coal at $\dot{\varepsilon}=2.0\ s^{-1}$.

Direction	Specimen	$\varepsilon_{fo}\times10^{-3}$	σ_{fo}[MPa]	$\varepsilon_{fm}\times10^{-3}$	σ_{fm}[MPa]	Average values
Z	2Z1	11.4	24.7	18.8	32.7	$\bar{\varepsilon}_{fo}=11.31\times10^{-3}$
	2Z3	12.8	21.0	18.6	27.1	$\bar{\sigma}_{fo}=26.58$[MPa]
	2Z4	11.3	31.0	18.6	40.1	$\bar{\varepsilon}_{fm}=18.43\times10^{-3}$
	2Z6	8.9	23.4	16.3	28.5	$\bar{\sigma}_{fm}=33.07$[MPa]
	2Z7	14.5	39.2	20.7	43.5	
	2Z8	9.0	20.2	17.6	26.5	

Because of the relatively short loading time, all process of compression was recorded with the aid of two digital transient recorders. Both the displacement in the form of an analog signal from the *DCDT*, and the force from the testing machine load cell, were recorded as a function of time; i.e. two independent recordings were obtained: $\delta(t)$ and $P(t)$. The independent recording enabled time to fracture to be determined. On the average, the time from the beginning of loading to fracture was $t_m = 23.7$ ms. A typical record from such a test is shown in Fig. 6.

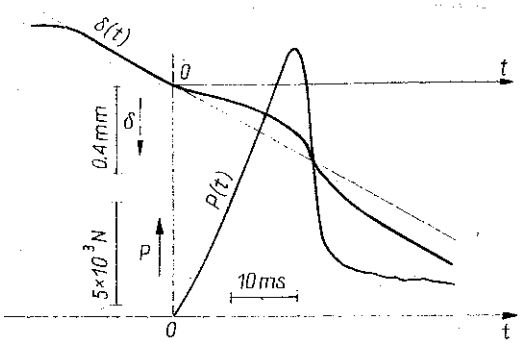

FIG. 6. A typical record of compression test on coal at strain rate $\dot{\varepsilon} \approx 2.0\ s^{-1}$.

It is interesting to note that the true strain rate, represented by an average slope of the $\delta(t)$ trace, is almost half of that programmed by the pulse generator of the testing machine, represented by a slope indicated by the broken line. This is caused by the very small displacement needed to crush a coal specimen, and proves the importance of using the *DCDT* system in displacement measurements.

After elimination of time, $\delta(P)$ plots could be obtained, and as a next step the compliance function was subtracted, thus providing stress-strain diagrams. This procedure was applied to all six specimens tested at $\dot{\varepsilon} \approx 2.0\ s^{-1}$.

These three strain rates complete tests on coal at low and intermediate rates. This is the largest possible rate range for a closed loop machine. In the present case the ratio of the highest to the lowest strain rate is

$$r = \frac{2.0}{1.3 \times 10^{-4}} = 1.54 \times 10^4.$$

Thus four orders of rate have been covered by these tests.

3. PROPERTIES OF COAL UNDER IMPACT LOADING

The study of the dynamic behaviour of coal has important applications in coal mining and blasting. There is not, however, a simple procedure developed so far to test coal under impact loading.

The procedure loading to the so-called Impact Strength Index [1] is based on degradation of coal fragments by a succession of drop-hammer blows. The I.S.I. test procedure may be defined as a technological one, and it does not lead to a strict definition of coal resistance to fracture under impact loadings.

Although there are attempts to correlate empirically the I.S.I. number and quasi-static uniaxial strength σ_f, this correlation does not provide any information about the behavior of coal under impact loading.

One of the modern techniques developed at Sandia Laboratories, U.S.A., is based on measurements of the response of coal under shock compression [2]. In this method a thin plate or cylindrical specimen of 28.6 mm diameter and 15 mm to 30 mm thick is shock loaded by a high velocity impact induced by a flat projectile. The free surface motion of the shocked specimen (the face of the specimen opposite the face impact), which is recorded with a high precision by a laser interferometry system, provides the shock wave profile correlated in turn to material behavior under uniaxial strain conditions. This experimental technique is widely used to test responses of metals under shock loading [7]. The technique itself is very costly, needs a large diameter fast gas gun, a large vacuum chamber, and a sophisticated system of electronic measurements, including a high power laser system and optics.

Another method of dynamic testing of materials in uniaxial compression (uniaxial stress) is the Hopkinson split-bar technique, see for example [8, 9, 10]. This test technique was initially developed for the testing of metals at high strain rates of about $10^3\ s^{-1}$. Later the technique found application in the testing of rocks, for example [11, 12, 13]. A more extensive review of existing literature on this technique is given in references [14–24].

Originally this method was proposed in 1949 by KOLSKY [16] to test materials in compression at very high strain rates. A more detailed history of its development can be found in [8, 17]. Although Hopkinson pressure have been used in different experimental configurations, the Kolsky apparatus has found the most widespread use. A newer version of the apparatus with three bars and two strain gage stations, instead of capacitance transducers, has been proposed by LINDHOLM [18]. This latest version offers the greatest capabilities in compression impact testing [19].

Theoretical analysis as well as numerical calculations have shown conclusively that the split-bar technique provides reliable information concerning dynamic stress-strain data [21, 23, 24].

However, there are certain limitations of the technique when applied to the testing of rocks and rock-like materials, including coal. To date several attempts have been reported in the literature on the use of the Hopkinson split-bar technique for dynamic testing of rocks. Early reports indicated the usefulness of the method [11, 12, 25, 26, 27]. All papers demonstrated high strain rate sensitivity of compression fracture stress for rocks [13, 28, 29, 30]. Application of the Hopkinson split-bar apparatus for dynamic testing of rocks has also been discussed in [31]. Recently this technique was applied to collect dynamic fracture and fragmentation data on oil shale [32, 33, 34]. Consequently, the natural way to test coal under impact is to apply directly the Hopkinson split-bar concept. An effort was undertaken at the Department of Mechanical Engineering at the University of Manitoba to design and construct the system. The system utilized is described wit more details in [6]. The impact velocities were achieved by using a pneumatically driven projectile (striker bar) of proper length, guided by a long launch tube. Besides the gas gun,

the experimental set-up consists of a system of two properly instrumented bars, and the measuring and recording equipment.

The system was specially designed to test coal, and eventually rocks, under impact loading. All bars are made of hard aluminium alloy (2024-T3 Alcan) of a diameter $D=38$ mm, Young's modulus $E=7.3\times10^4$ MPa, and yield point (0.2% offset) $\sigma_y=312$ MPa.

4. Stress–strain characteristics of coal determined from impact experiments

High strain rate tests at two strain rates, approximately $\dot{\varepsilon}_f\approx150\ s^{-1}$ and $\dot{\varepsilon}_f\approx2000\ s^{-1}$, were performed with the Hopkinson split-bar apparatus. The same specimen geometry and lubricant was employed as for the quasi-static tests.

The results for the lower strain rate series are shown in Fig. 7 (series 3Z), the loading direction is again Z.

It has been observed that stress-strain characteristics determined from the Hopkinson split bar technique at the lower strain rates are quite similar to those obtained

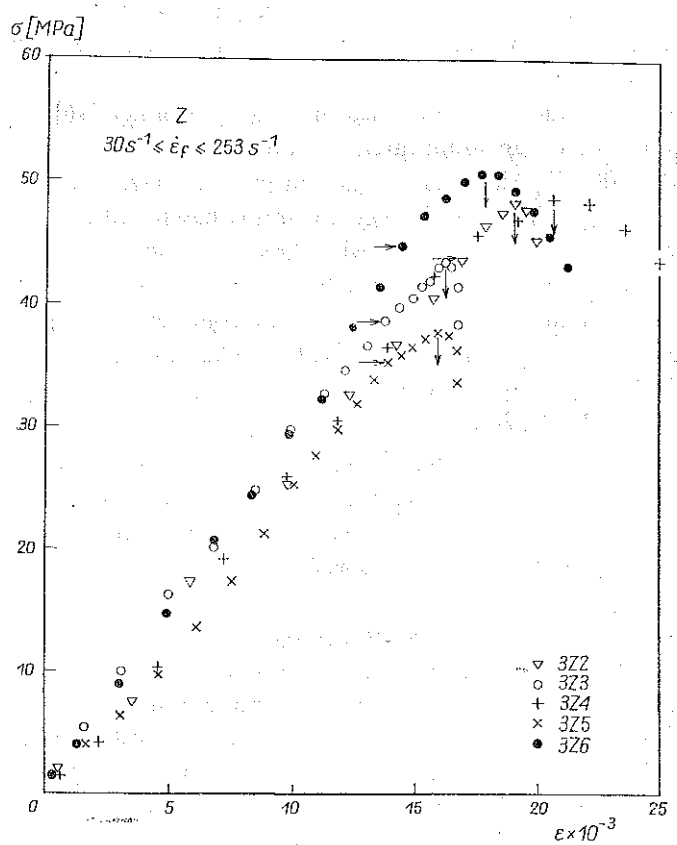

Fig. 7. Stress-strain curves for lover strain rate region 30 $s^{-1}\leqslant\dot{\varepsilon}_f\leqslant253\ s^{-1}$, (series 3Z) loading in Z direction.

from quasi-static loading. However, a small rate effect is observed, with values of σ_f generally higher than for quasi-static loading. All characteristic values obtained during the course of this series of tests are given in Tables 4 and 5. It is shown in these tables that the average time to fracture is $t_f \approx 118$ μs, and the strain rate during fracture is within the range $30\ s^{-1} \leqslant \dot{\varepsilon}_f \leqslant 253\ s^{-1}$. The fracture stress $\sigma_f = 45.46$ MPa, is slightly higher than for the quasi-static tests. However, a definite trend of increasing maximal strain at fracture ε_f is observed.

Table 4. Crushing parameters for coal in Z direction, as determined from the split Hopkinson bar test — — lower strain rates; σ_{fo} and σ_{fm}. $30s^{-1} \leqslant \dot{\varepsilon}_f \leqslant 253\ s^{-1}$

Direction	Specimen	t_f[μs]	$\dot{\varepsilon}_f$[s^{-1}]	σ_{fo}[MPa]	σ_{fm}[MPa]
Z	3Z2	137.5	37.2	45.5	48.1
	3Z3	143.4	30.6	38.5	43.2
	3Z4	65.9	252.9	42.0	48.4
	3Z5	152.9	51.5	35.2	37.6
	3Z6	90.3	118.1	44.6	50.0
Z	Average	118.0	98.1	40.76	45.46
				$s=3.87$	$s=5.08$

s—standard deviation

Table 5. Crushing parameters for coal in Z direction, as determined from the split Hopkinson bar test — — lower strain rates; ε_{fo} and ε_{fm}. $30s^{-1} \leqslant \dot{\varepsilon}_f \leqslant 253\ s^{-1}$

Direction	Specimen	t_f[μs]	$\dot{\varepsilon}_f$[s^{-1}]	$\varepsilon_{fo} \times 10^{-3}$	$\varepsilon_{fm} \times 10^{-3}$
Z	3Z2	137.5	37.2	16.8	19.0
	3Z3	143.4	30.6	13.7	16.1
	3Z4	65.9	252.9	15.7	20.6
	3Z5	152.9	51.5	13.8	15.8
	3Z6	90.3	118.1	16.4	17.6
Z	Average	118.0	98.1	15.28	17.82
				$s=1.45$	$s=2.01$

s—standard deviation

The results for the second series of tests using the Hopkinson split bar apparatus are shown in Fig. 8 (series 4Z). This series was completed with the highest possible strain rate acceptable with respect to the specimen gemoetry. However, in this case the time to fracture is very short (approximately 26.4 μs) and stress equilibrium across the specimen may not be achieved in this time interval. Therefore, inertial forces may influence the amplitude of the transient peak stress recorded as proportional to the peak of the transmitted pulse $\varepsilon_T(t)$. Fracturing will tend to attenuate the amplitude of a propagating pulse across the specimen and reduce the transmitted stress as considered in [12]. Because the total mass of the coal speci-

men is relatively low, an equivalent inertial stress produced is assumed to be negligible. A further discussion of the inertial effects associated with this experimental technique, though present in the literature [16, 21], is beyond the scope of this

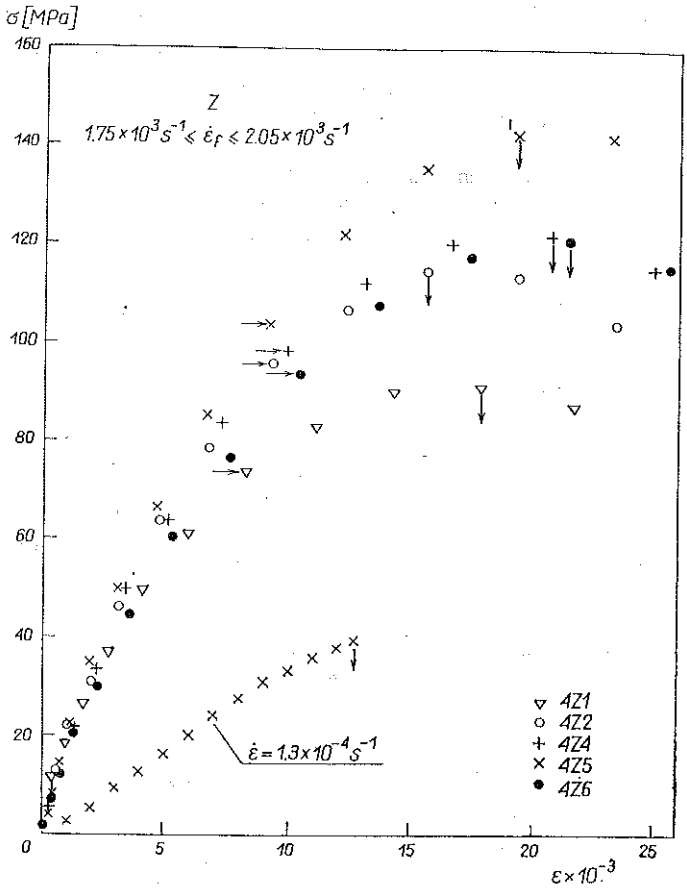

FIG. 8. Stress-strain curves for high strain rate region $1.75\times10^3\ s^{-1}\leqslant\dot{\varepsilon}_f\leqslant2.05\times10^3\ s^{-1}$, also average stress-strain curve is shown at $\dot{\varepsilon}=1.3\times10^{-4}\ s^{-1}$.

paper. Generally there is a degree of uncertainty in the interpretation of fracture stress data for brittle materials using the Hopkinson split-bar technique at very high loading rates.

All parameters obtained during the series of tests at the highest strain rates are given in Tables 6 and 7. Both Fig. 8 and Table 7 reveal a substantial rate effect for coal within the high strain rate region attained, $1.75\times10^3\ s^{-1}\leqslant\dot{\varepsilon}_f\leqslant2.05\times10^3\ s^{-1}$. To demonstrate the magnitude of the strain rate influence the quasi-static average stress-strain diagram for $\dot{\varepsilon}\approx1.3\times10^{-4}\ s^{-1}$ has also been shown in Fig. 8. The dynamic to quasi static ratio of $\bar{\sigma}_{f0}$ and $\bar{\sigma}_f$ can be calculated from comparison of Tables 1 and 6 as

$$\frac{(\bar{\sigma}_{f0})_{dyn}}{(\bar{\sigma}_{f0})_{stat}}=\frac{93.24}{31.94}=2.92,\qquad \frac{(\bar{\sigma}_f)_{dyn}}{(\sigma_f)_{stat}}=\frac{120.52}{39.92}=3.02.$$

Thus the ratio of dynamic to quasi-static crushing stress for coal in the Z direction is approximately three. In addition, the fracture strain ε_f is larger for dynamic loading conditions than that observed during quasi-static tests, having a ratio of

$$\frac{(\bar{\varepsilon}_f)_{\text{dyn}}}{(\bar{\varepsilon}_f)_{\text{stat}}} = \frac{1.89\times10^{-2}}{1.268\times10^{-2}} = 1.49.$$

Table 6. Crushing parameters for coal in Z direction, as determined from the split Hopkinson bar test — — the highest strain rates; σ_{fo} and σ_{fm}.
$1.75\times10^3 s^{-1} \leqslant \dot{\varepsilon} \leqslant 2.05\times10^3 s^{-1}$

Direction	Specimen	t_f[μs]	$\dot{\varepsilon}_f$[s^{-1}]	σ_{fo}[MPa]	σ_{fm}[MPa]
Z	4Z1	26.0	1852	73.8	103.6
	4Z2	24.0	1746	96.0	114.5
	4Z4	28.0	2046	98.7	121.8
	4Z5	28.0	1920	103.9	142.1
	4Z6	26.0	2050	93.8	120.6
Z	Average	26.4	1922.8	93.24	120.52
				s=11.50	s=14.05

s—standard deviation

Table 7. Crushing parameters for coal in Z direction, as determined from the split Hopkinson bar test — — the highest strain rates; ε_{fo} and ε_{fm}.

Direction	Specimen	t_f[μs]	$\dot{\varepsilon}_f$[s^{-1}]	$\varepsilon_{fo}\times10^{-3}$	$\varepsilon_{fm}\times10^{-3}$
Z	4Z1	26.0	1352	8.3	17.8
	4Z2	24.0	1746	9.3	15.6
	4Z4	28.0	2046	10.0	20.6
	4Z5	28.0	1920	9.2	19.2
	4Z6	26.0	2050	10.4	21.3
Z	Average	26.4	1922.8	9.5r	18.90
				s=0.81	s=2.28

s — standard deviation

All representative stress-strain curves which are given in Fig. 8 indicate the substantial effect of strain rate on both fracture stress σ_f and fracture maximum strain ε_f. The experimental points are shown only up to strains slightly in excess of maximum stress. For the high strain rate tests some relaxation time is observed to decay the stress from the maximum level. Generally, the stress-strain curves obtained at a strain rate $\sim 2\times10^3\ s^{-1}$ show a parabolic shape rather than the typical S-shape.

5. The strain rate spectrum for crushing of coal

Since crushing of coal is generally found to be sensitive to the rate of deformation, this rate sensitivity can be demonstrated as a function of strain rate. Test results from a variety of rocks show a strong dependence of the ultimate or fracture strength on both rate of deformation and temperature. In addition, radial confining pressure (the hydrostatic component of the stress tensor) affects substantially the fracture strength [14]. Thus a general formulation of the fracture condition for a uniaxial stress should be a function of the following parameters:

$$\sigma_f^+ = f(\varepsilon_f^+, \dot{\varepsilon}_f^+, T, p)_V,$$

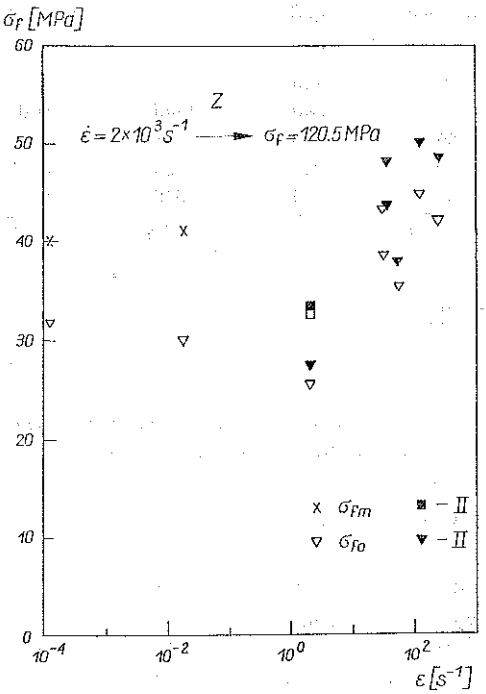

FIG. 9. Strain rate spectra for coal in compression ▽, □ — denotes σ_{fo}, ×, ■, ▼ — denotes σ_{fm}; ▼ — σ_{fm} from Hopkinson split-bar test.

where σ_f^+ is the crushing stress in compression for a particular volume V of a specimen material, ε_f^+ and $\dot{\varepsilon}_f^+$ denote respectively the fracture strain and the strain rate at fracture (maximal stress), T is temperature and p hydrostatic pressure. A similar surface of four parameters $(\varepsilon_f^-, \dot{\varepsilon}_f^-, T, p^-)$ can be constructed in tension to describe changes of σ_f. This type of fracture criterion for uniaxial compression of Dresser basalt was discussed in [13]. A similar criterion should be derived for coal. On the basis of quasi-static and Hopkinson split-bar results, the following strain rate spectra can be constructed: $\sigma_{fo}(\log \dot{\varepsilon})_{\varepsilon_{fo}}$ and $\sigma_{fm}(\log \dot{\varepsilon}_i)_{\varepsilon_{fm}}$, both at atmospheric pressure, room temperature $T \approx 300$ K, and constant specimen volume V.

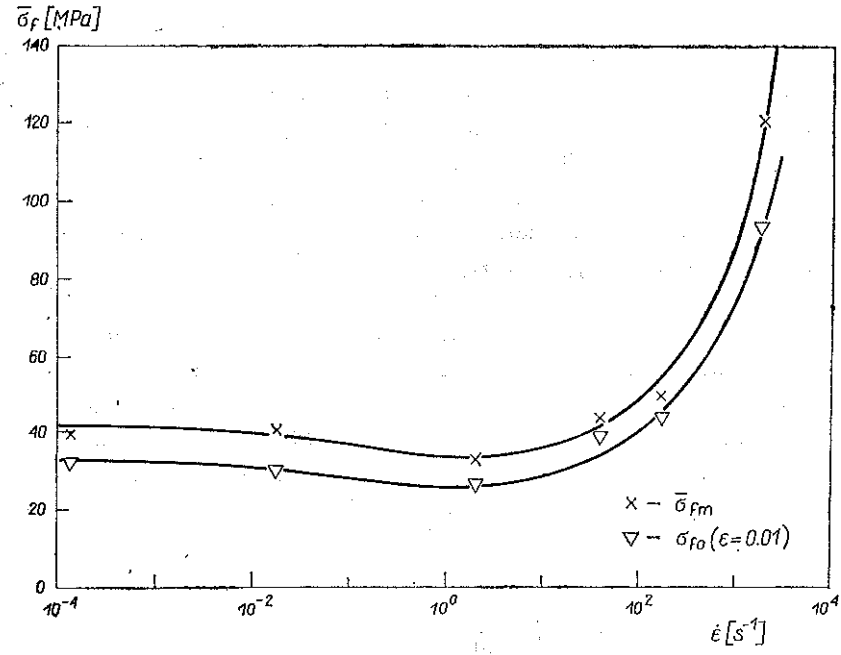

FIG. 10. Complete strain rate spectra for coal in compression, mean values of σ_{f0} — ∇ and σ_{fm} — ×.

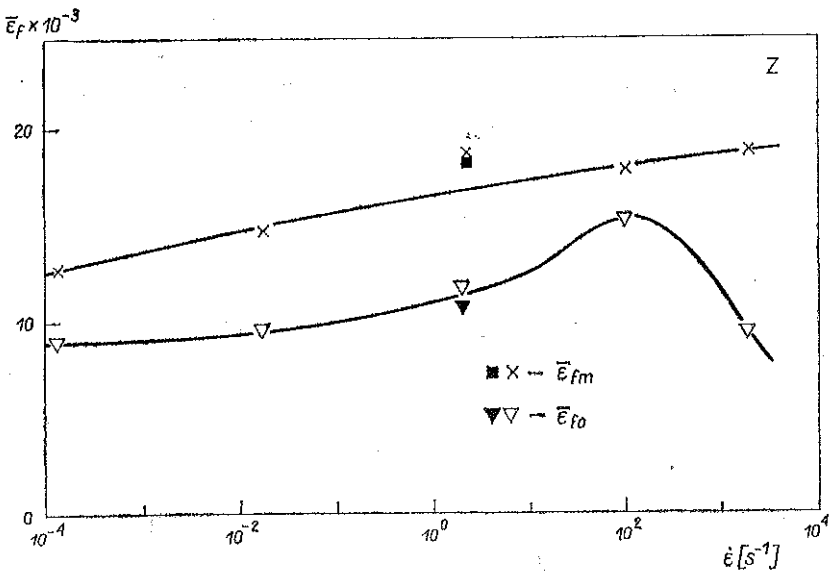

FIG. 11. Strain rate spectra for coal at fracturing strain $\bar{\varepsilon}_{f0}$ — ∇, ▼ and $\bar{\varepsilon}_{fm}$ — ×, ■; at $\dot{\varepsilon} \approx 2\ s^{-1}$ two series of tests have been performed.

These spectra are shown in Figs. 9 and 10. Points for the three lower strain rates are the mean values, whereas Hopkinson split-bar data show σ_{f0} and σ_{fm} for each specimen. Values of σ_{f0} and σ_{fm} for the highest strain rate are not shown in Fig. 9. The full spectrum of mean values $\bar{\sigma}_f$ is shown in Fig. 10. It may be concluded that the strain rate sensitivity for fracturing of coal is highly nonlinear.

Up to the strain rate $\dot{\varepsilon} \approx 50\ \mathrm{s}^{-1}$ a plateau is observed, or even a minimum may occur at $\dot{\varepsilon} \approx 10\ \mathrm{s}^{-1}$. At the high strain rate region rate sensitivity increases dramatically and σ_f is much higher than the plateau level. Such a trend is observed for both fracture stresses, i.e. σ_{f0} and σ_{fm}.

A different strain rate spectrum is observed for mean fracture strains $\bar{\varepsilon}_{f0}$ and $\bar{\varepsilon}_{fm}$. Such a spectrum is shown in Fig. 11. It is observed that both quantities $\bar{\varepsilon}_{f0}$ and $\bar{\varepsilon}_{fm}$ increase during increase of strain rate, but $\bar{\varepsilon}_{f0}$ shows a maximum at $\dot{\varepsilon} \approx 100\ \mathrm{s}^{-1}$ and then decreases. Values of $\bar{\varepsilon}_{fm}$ show a tendency to increase within the entire range of the applied strain rates, i.e. $10^{-4}\ \mathrm{s}^{-1} \leqslant \dot{\varepsilon} \leqslant 2 \times 10^{3}\ \mathrm{s}^{-1}$, or over seven decimal orders. Again Fig. 11 demonstrates the very complicated behavior of coal under compression impact.

6. Discusion and conclusions

The experimental techniques developed during the course of the coal testing seem to be very useful in characterizing the behavior of this material over a wide range of strain rates. The quasi-static technique of precision compression testing makes it possible to measure stress-strain diagrams for coal with a high resolution and at a variety of lower strain rates up to $\dot{\varepsilon}$—$10\ \mathrm{s}^{-1}$. For example, this technique may be useful in determining of the Strain Energy Storage Index [35] for different strain rates. The Strain Energy Storage Index for coal is the simplest rock-burst liability indicator. This index is defined as the ratio of the energy released W_e (elastic strain energy) to the disspated energy W_d during one loading—unloading loop, possibly close to the σ_f. According to this definition, the Strain Energy Storage Index κ is, [35, 36, 37],

$$\kappa = \frac{W_e}{W_d},$$

where

$$W_e \int_{\varepsilon_p}^{\varepsilon_0} \sigma(\varepsilon^-)\, d\varepsilon \quad \text{for unloading}$$

and

$$W_d = \int_0^{\varepsilon_0} \sigma(\varepsilon^+)\, d\varepsilon - \int_{\varepsilon_p}^{\varepsilon_0} \sigma(\varepsilon^-)\, d\varepsilon,$$

An average value for SESI for quasi-static loading is $\kappa \approx 5$, [35]. It is obvious, in light of the present results, that the index κ must be strongly rate dependent and rather should be determined under impact loading. A further discussion of this problem is beyond the scope of this paper.

The split Hopkinson pressure bar technique, as applied to impact loading of coal, offers more possibilities to achieve strain rates up to 2000 s^{-1} than by any other method.

A series of quasi-static tests at $\dot{\varepsilon}=1.3\times10^{-4}\,s^{-1}$ for three different loading directions have indicated that the coal tested can be characterized to some extent. as having transverse isotropy. This type of anisotropy is such that the material is isotropic in the (XY) (bendding) plane, and anisotropic in any other combination of planes, including Z—the strongest direction.

Measurements of stress-strain diagrams for all three directions of loading indicate that an S-shape is always observed when a proper gain of strain reading is set. Thus, it is the typical feature of coal.

Dynamic measurements indicate in addition that the elastic properties of coal are time dependent and, consequently, as attempted in [1], a viscoelastic model of material behavior should be employed for further analysis.

The high stress region is characterized by a kind of "strain hardening" and a permanent deformation, probably having its source in microcracking. This part of the stress-strain diagram is also highly rate sensitive, especially over the high strain rate region. Thus, in addition to viscoelasticity a "viscoplastic" behavior is observed.

Finally, the crushing stress σ_f is also rate sensitive over a high strain rate region, which would lead to the formulation of a rate and perhaps temperature dependent fracture criterion.

The present study of the mechanical behavior of coal specimens in compression was performed only at one specimen size, i.e. discs of $l_0=12.5$ mm and $D\cong25$ mm. Due to the relatively small volume of such specimens, all generalizations of the present results must consider the effect of volume [1, 38]. It is known, for example, that the crushing strength of coal decreases as specimen volume increases. This observation leads to the conclusion that the volume function should be derived by a statistical method, for example [1, 38, 29].

Acknowledgement

The author is indebted to Drs. T. R. Hsu and N. M. Bassim of the Department of Mechanical Engineering, The University of Manitoba, for the invitation to participate in the research project "On Fracture and Thermal Conditioning of Canadian Coals" granted by the Natural Science and Engineering Research Council of Canada under grant No. G-0459. Thanks are due also to Mssrs. D. Fedorovich and D. Kuss for their skillful assistance during the construction of equipment (Hopkinson split-bar) and specimen preparation.

References

1. I. Evans, C. D. Pomeroy, *The strength fracture and workability of coal*, Pergamon Press, Oxford 1966.
2. B. M. Butcher, A. L. Stevens, *Shock wave response of window rock coal*, Int. J. Rock Mech. Min. Sci. and Geomach. Abstr., **12**, 147, 1975.

3. M. S PATERSON, *Experimental rock deformation, the brittle field*, J., Springer, 1978.
4. J. C. YAEGER, N. G. W. COOK, *Fundamentals of rock mechanics*, A. Halsted Press Book, 2nd ed., Chapman and Hall, 1976.
5, *The determination of physical mechanical and fracture properties of coal*, Coal Research Group, Department of Mechanical Engineering, University of Manitoba, November, 1981,
6. J. R. KLEPACZKO, *Quasi-static and dynamic compression behavior of coal*, Technical Report, Dept. of Mech. Eng. The University of Manitoba, March, 1982.
7. L. M. BARKER, R. E. HOLLENBACH, *System for measuring the dynamic properties of materials*, Rev. Sci. Instr., **35**, 742, 1964.
8. H. KOLSKY, *Stress waves in solids*, Dover Publ., 1963.
9. U. S. LINDHOLM, *High strain rate tests*, in: Techniques in Metals Research, ed. R. Bunshach, Vol. 5, Interscience, 1971.
10. U. S. LINDHOLM, L. M. YEAKLEY, *High strain-rate testing: tension and compression*, Exp. Mech., **8**, 1, 1968.
11. P. B. ATTEWEL, *Response of rocks to high velocity impacts*, Bull. Inst. Min. Met., 705, 1962.
12. K. O. HAKALEHTO, *Brittle fracture of rocks under impulse loads*, Int. J. Fracture Mech., **1**, 311, 1965.
13. U. S. LINDHOLM, L. M. YEAKLEY and A. NAGY, *The dynamic strength and fractue properties of dresser basalt*, Int. J. Rock Mech., Min. Sci. and Geomech Abstr., **11**, 181, 1974
14. B. HOPKINSON, *A method of measuring the pressure produced in the detonation of high explosives and by the impact of bullets*, Phil. Trans. Roy. Soc. (London), Ser. A, **213**, 437, 1914.
15. R. M. DAVIES, *A critical study of the Hopkinson pressure bar*, Phil. Trans. Roy. Soc. (London), Ser. A, **240**, 375, 1948.
16. K. KOLSKY, *An investigation of the mechanical properties of materials at very high rates of loading*, Proc. Phys. Soc. (London), Ser. B, **62**, 676, 1964.
17. F. E. HAUSER, *Techniques for measuring stress-strain relations at high strain rates*, Experimental mechanics, **6**, 395, 1966.
18. U. S. LINDHOLM, *Some experiments with split Hopkinson pressure bar*, J. Gech. Phys. Solids, **12**, 317, 1964.
19. J. KLEPACZKO, *The modified split Hopkinson bar*, Mech, Teoret. i Stos., **9**, 471, 1971 [in Polish].
20. C. J. MAIDEN, S. J. GREEN, *Compression strain-rate tests on six-selected materials at strain rates from* 10^{-3} *to* 10^{-4} *in/in/sec*, J. Appl. Mech., **33**, 496, 1966.
21. E. D. H. DAVIES, S. C. HUNTER, *The dynamic compression testing of solids by the method of split Hopkinson pressure bar*, U. Mech, Phys. Solids, **11**, 155, 1963
22. E. W. BILLINGTON, C. BRISSENDEN, *Mechanical properties of various polymeric solids tested in compression* Int. J. Mech. Sci., **13**, 531, 1971.
23 W. E. JAHSMAN *Reexamination of the Kolsky technique for measuring dynamic material behaviour*. J. Appl. Mech., **41**, 137, 1974
24. L. D. BERTHOLF, C. H. KARMES, *Two-dimensional analysis of the split Hopkinson pressure bar system*, J. Mech. Phys. Solids., **23**, 1, 1975.
25. A. KUMAR, *The effect of stress rate and temperature on the strength of basalt and granite*, Geophysics, **33**, 501, 1968.
26. S. J. GREEN, R. D. PERKINS, *Uniaxial compression tests at strain rates from* 10^{-4}*/sec to* 10^{-4}*/sec on three geological materials*, Proc. Tenth Symp. on Rock Mech., 1968.
27. E. D. PERKINS, S. J. GREEN, M. FRIEDMAN, *Uniaxial stress behavior of porphyritic tomalite at strain rates to* 10 */second*, Int. J. Rock Mech. Min. Sci., **7**, 527, 1970.
28. B. LUNDBERG, *A split Hopkinson bar study of energy absorption in dynamic rock fragmentation*, Int. J. Rock Mech. Min. Sci., **13**, 187, 1976.
29. R. J. CHRISTENSEN, S. R. SWANSON, W. S. BROWN, *Split Hopkinson bar tests on rock under confining pressure*, Exp. Mech. **12**, 508, 1972.

30. J. BUCHER, Z. BILEK. *Application of the split bar test to the mechanical and fracture properties of rocks, fracture mechanics methods for ceramics, rocks and concrete*, ASTM STP 745, Pennsylvania, 185, 1981.
31. J. KLEPACZKO, *Application of the modified split Hopkinson pressure bar for impact testing of rocks*, Engineering Transactions, 1980.
32. W. JAHSMAN, *Dynamic fracture strength of oil shale and coal*, University of Oxford Engineering Lab. Report No. 1295, Oxford 1979.
33. D. E. GRADY, M. E. KIPP, *Oil shale fracture and fragmentation at high rates of loading*, Sandia Laboratories, Rep No SAND-79-05630, Albuquerque 1979.
34. M. J. FORRESTAL, D. E. GRADY, K. W. SCHYLER, *An experimental method to estimate the dynamic fracture strength of oil shale in the* 10^3 *to* 10 s^{-4} *strain rate regime*, Int. J. Rock Mech. Min. Sci., **15**, 263, 1978.
35. A. KIDYBIŃSKI, *Bursting liability indices of coal*, Int. J. Rock Mech. Min. Sci. and Geomech. Abstr., **18**, 295, 1981.
36. W. BURGERT, H. LIPPMANN, *Models of translatory rock bursting in coal*, Int. J. Rock Mech. Min. Sci. and Geomech. Abstr., **18**, 285, 1981.
37. W, HUCKA, B. DAS, *Brittleness determination of rock by different methods*, Int. J. Rock Mech. Min. Sci., **11**, 389, 1974.
38. Z. T. BIENIAWSKI, *The effect of specimen size on compressive strength of coal*, Int. J. Rock Mech. Min. Sci., **5**, 325, 1968.
39. T. R. HSU, *Engineering design of brittle structures*, Rep. 80-2-70, Thermomechanics Laboratories, Dept. of Mechanical Engineering, The University of Manitoba.

STRESZCZENIE

O WRAŻLIWOŚCI WĘGLA KAMIENNEGO NA PRĘDKOŚĆ ODKSZTAŁCENIA

W pracy zawarto opis technik doświadczalnych w zakresie quasi-statycznym i dynamicznym, znajdujących zastosowanie w próbie ściskania węgla kamiennego w szerokim zakresie prędkości odkształcenia, od $\dot{\varepsilon}_{min} \approx 1. \times 10^{-4}$ s^{-1} do $\dot{\varepsilon}_{max} \approx 2 \times 10^3$ s^{-1}. W zakresie małych i średnich prędkości odkształcenia zastosowano maszynę wytrzymałościową z zamkniętą pętlą sterowania, natomiast badania w zakresie dużych prędkości odkształcenia zostały przeprowadzone na specjalnie skonstruowanym do tego celu zmodyfikowanym pręcie Hopkinsona. Kierunek obciążenia dla wszystkich badanych próbek ograniczono do kierunku prostopadłego do płaszczyzny złoża (kierunek *Z*). Wyniki badań uzyskane w zakresie dużych prędkości odkształcenia ($\dot{\varepsilon} \approx 10^3$ s^{-1}) wykazały bardzo silną zależność naprężenia inicjacji mikrospękania ε_{f0} oraz naprężenia niszczącego ε_{fm} od prędkości odkształcenia. W zakresie małych i średnich prędkości odkształcenia wytrzymałość węgla kamiennego w próbie ściskania wykazuje brak wrażliwości na prędkość odkształcenia.

Резюме

О ЧУВСТВИТЕЛЬНОСТИ КАМЕННОГО УГЛЯ НА СКОРОСТЬ ДЕФОРМАЦИИ

В работе содержится описание экспериментальных техник, в казистатической и динамической областях, находящих применение в испытании сжатия каменного угля в широком интервале скорости деформации, от $\varepsilon_{мин} \approx 1{,}3 \cdot 10^{-4}$ $с^{-1}$ до $\varepsilon_{макс} \approx 2 \cdot 10^3$ $с^{-1}$. В интервале малых и средних скоростей деформации применена испытательная машина с замкнутой петлей управления, исследования же в области больших скоростей деформации проведены на специально построенном для этой цели модифицированном стержне Гопкинсона

Направление нагружения для всех исследованных образцов ограничено к направлению перпендикулярному к плоскости месторождения (направление Z). Результаты исследований, полученные в интервале больших скоростей деформации ($\dot{\varepsilon} \approx 10^3\ \mathrm{c}^{-1}$), показали очень сильную зависимость напряжения инициирования микротрещины $\sigma_{f\,0}$ и разрушающего напряжения σ_{fm} от скорости деформации. В интервале малых и средних скоростей деформаций прочность каменного угля в испытании сжатия показывает отсутвие чувствительности на скорость деформации

POLISH ACADEMY OF SCIENCES
INSTITUTE OF FUNDAMENTAL TECHNOLOGICAL RESEARCH

Received December 6, 1982.